Natural Resources Canada
Ressources naturelles Canada

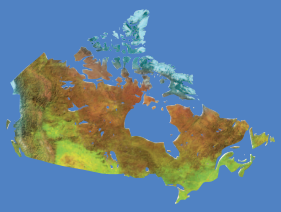

Airborne time-domain electromagnetic data for mapping and characterization of the Spiritwood Valley aquifer, Manitoba, Canada

G.A. Oldenborger, A.J.-M. Pugin, M.J. Hinton, S.E. Pullan, H.A.J. Russell, and D.R. Sharpe

Geological Survey of Canada

Current Research 2010-11

2010

Canada

Geological Survey of Canada
Current Research 2010-11

Airborne time-domain electromagnetic data for mapping and characterization of the Spiritwood Valley aquifer, Manitoba, Canada

G.A. Oldenborger, A.J.-M. Pugin, M.J. Hinton, S.E. Pullan, H.A.J. Russell, and D.R. Sharpe

2010

ISSN 1701-4387
Catalogue No. M44-2010/11E-PDF
ISBN 978-1-100-16633-9
doi:10.4095/286056

A copy of this publication is also available for reference in depository libraries across Canada through access to the Depository Services Program's Web site at http://dsp-psd.pwgsc.gc.ca

A free digital download of this publication is available from GeoPub: http://geopub.nrcan.gc.ca/index_e.php

Toll-free (Canada and U.S.A.): 1-888-252-4301

Recommended citation

Oldenborger, G.A., Pugin, A.J.-M., Hinton, M.J., Pullan, S.E., Russell, H.A.J., and Sharpe, D.R., 2010. Airborne time-domain electromagnetic data for mapping and characterization of the Spiritwood Valley aquifer, Manitoba, Canada; Geological Survey of Canada, Current Research 2010-11, 13 p.

Critical review
P. Keating
J. Hunter

Authors
G.A. Oldenborger
(Greg.Oldenborger@NRCan-RNCan.gc.ca)
A.J.-M. Pugin
(Andre.Pugin@NRCan-RNCan.gc.ca)
M.J. Hinton
(Marc.Hinton@NRCan-RNCan.gc.ca)
S.E. Pullan
(Susan.Pullan@NRCan-RNCan.gc.ca)
H.A.J. Russell
(Hazen.Russell@NRCan-RNCan.gc.ca)
D.R. Sharpe
(David.Sharpe@NRCan-RNCan.gc.ca)
Geological Survey of Canada
601 Booth Street
Ottawa, Ontario
K1S 0L8

Correction date:

Airborne time-domain electromagnetic data for mapping and characterization of the Spiritwood Valley aquifer, Manitoba, Canada

G.A. Oldenborger, A.J.-M. Pugin, M.J. Hinton,
S.E. Pullan, H.A.J. Russell, and D.R. Sharpe

Oldenborger, G.A., Pugin, A.J.-M., Hinton, M.J., Pullan, S.E., Russell, H.A.J., and Sharpe, D.R., 2010. Airborne time-domain electromagnetic data for mapping and characterization of the Spiritwood Valley aquifer, Manitoba, Canada; Geological Survey of Canada, Current Research 2010-11, 13 p.

Abstract: A helicopter-borne, time-domain electromagnetic survey was flown over a 1062 km^2 area of the Spiritwood Valley in southern Manitoba. The objective was to test the effectiveness of commercial, airborne, time-domain electromagnetics for mapping and characterizing buried valley aquifers in the Canadian Prairies. The preliminary data exhibit rich information content, but show some levelling bias and potential limitations of dynamic range or bandwidth. Time slices of the magnetic field decay clearly map the broader Spiritwood Valley in addition to a continuous, incised valley along the broader valley bottom. The data indicate a complex valley morphology with nested scales of valleys, including at least three distinct valley features and multiple possible tributaries. Time-domain electromagnetic response magnitude and decay rates indicate that the fill material within the incised valleys is more resistive than the broader valley fill, consistent with an interpretation of sand and gravel. The electromagnetic data are in excellent agreement with seismic reflection data collected inside the survey block. Further ground-based investigation and data integration is planned. These preliminary results suggest that time-domain electromagnetic surveys have the potential for mapping buried valley aquifers in the Canadian Prairies in far greater detail that any previous techniques.

Résumé : Un levé électromagnétique dans le domaine du temps a été effectué par hélicoptère au-dessus de la vallée de Spiritwood (sud du Manitoba), couvrant une superficie de 1062 km^2. L'objectif consistait à évaluer l'efficacité de systèmes commerciaux aéroportés pour effectuer des levés aéromagnétiques dans le domaine du temps afin de cartographier et caractériser des aquifères de vallée enfouie dans les Prairies canadiennes. Les données provisoires offrent un riche contenu informatif, mais peuvent présenter des erreurs systématiques de nivellement et comporter des limites quant à la plage dynamique ou la largeur de bande. Les tranches de temps de la décroissance du champ magnétique produisent une image claire de la vallée de Spiritwood, ainsi que d'une vallée encaissée continue qui suit le fond de cette vallée plus évasée. Les données indiquent une morphologie de vallée complexe comportant des écailles de vallées emboîtées qui comprennent au moins trois entités (vallées) distinctes et plusieurs tributaires possibles. L'intensité et les taux de décroissance de la réponse électromagnétique dans le domaine du temps indiquent que les matériaux de remplissage des vallées encaissées sont plus résistifs que ceux de la vallée plus large, en accord avec l'interprétation selon laquelle il s'agirait de sable et de gravier. Les données électromagnétiques concordent très bien avec les données de sismique-réflexion acquises dans le secteur du levé. On prévoit effectuer d'autres travaux de recherche au sol et procéder à l'intégration des données. Ces résultats provisoires suggèrent que les levés électromagnétiques dans le domaine du temps offrent la possibilité de cartographier les aquifères de vallée enfouie dans les Prairies canadiennes de façon beaucoup plus détaillée que ne le permettait toute autre méthode jusqu'à présent.

INTRODUCTION

Buried valleys occur across the glaciated terrains of Canada, the northern United States, and northern Europe. Where filled with coarse-grained, permeable sediments, these valleys represent potential sources of groundwater. Productive buried valley aquifers are common in Canada, yet knowledge of their distribution and groundwater resource potential is inadequate (Russell et al., 2004). Systematic mapping and resource evaluation of buried valleys is hindered by the lack of surface expression, longitudinal and cross-sectional variability, and complicated network geometries. As quasi-linear km-scale features, buried valleys represent preferential flow paths that may have significant influence on regional groundwater flow regimes, but may go unmapped or uncharacterized in traditional hydrogeological studies (e.g. Shaver and Pusc, 1992; Abraham et al., 2010).

Basin analysis methods foster understanding of buried valley aquifers via a predictive framework of their spatial and stratigraphic nature (e.g. Sharpe et al., 2002). However, with respect to characterization of buried valleys, it is difficult to map valley extent and the nature of the valley fill at a regional scale in the absence of spatially continuous data (Jørgensen and Sandersen, 2009). Ground-based methods of subsurface investigation such as boreholes, pump tests, or two-dimensional geophysics provide localized information for conceptual model development, but are not suitable for detailed regional mapping.

Airborne geophysics can provide rapid, high-resolution data acquisition at regional scales not amendable to ground surveys. Airborne electromagnetic (AEM) experiments are appropriate in groundwater exploration because of the well-known dependence of electrical conductivity on water content and lithology. When tied to ground truth such as high-quality boreholes or ground geophysics, AEM can be used to extrapolate knowledge on a regional scale, thereby capturing the complicated network of buried valleys as well as testing conceptual models. Once methodology and context are established, AEM can be used for large-scale regional mapping.

Successful application of AEM to the mapping and characterization of buried valleys has been demonstrated in Germany (Gabriel et al., 2003; Steuer et al., 2009), Denmark (Auken et al., 2008) and, to a lesser extent, the United States (Smith et al., 2010). Application to the Canadian landscape requires additional research. Although the buried valleys may share a common morphology and origin, the geological context and the resulting electrical properties are different. Furthermore, depths of buried valleys across Canada will largely require time-domain AEM systems, and commercial time-domain AEM instrumentation has been developed almost exclusively in a mineral exploration context (Sørensen and Auken, 2004). Applicability of these systems for regional mapping of near-surface resistive materials has yet to be soundly established both in terms of target identification, data collection, and processing (e.g. Martinez et al., 2008).

Commercial Canadian time-domain AEM systems have been utilized in groundwater studies for salinity mapping (e.g. Smith et al., 2004) and airborne contractors advertise results for groundwater prospecting in arid environments. However, these examples represent detection/location of a conductive target in a variably resistive host with strong contrast. We consider this to be distinct from the more general demands of resistivity mapping where the definition of target and host become blurred, often with weak contrasts and/or the host being the more conductive material. One example of a comparable survey is presented by Walker and Rudd (2008) in the context of oil sands exploration.

To test the applicability of airborne electromagnetics for the mapping and characterization of buried valley aquifers in Canada, a helicopter time-domain electromagnetic survey was carried out over the inferred region of the Spiritwood Valley in southern Manitoba. This aquifer represents a municipal and rural source of groundwater (Wiecek, 2009) and is trans-boundary in nature with the state of North Dakota (Randich and Kuzniar, 1984). This study represents one of the first applications of helicopter time-domain electromagnetics to aquifer mapping in Canada; preliminary results demonstrate significant value for aquifer mapping, characterization, resource management, and basin analysis models that may be applicable country-wide.

GEOLOGICAL SETTING

The Spiritwood Valley is a buried bedrock valley that runs approximately northwest-southeast near the towns of Killarney and Cartwright and extends 500 km from Manitoba, across North Dakota and into South Dakota (Winter et al., 1984). A number of buried valleys are known to exist in southwestern Manitoba (Betcher et al., 2005), but the extent and characteristics of the Spiritwood Valley aquifer in Manitoba are not fully defined.

The current study area extends from the Canada–USA border to northwest of Killarney, Manitoba within a till plain of little topographic relief. In this area, the bedrock valley has been identified and geographically constrained primarily based on water well information (Fig. 1; Wiecek, 2009). In North Dakota, the valley has been defined by a series of borehole transects to be up to 15–20 km wide and 100–150 m deep (Bluemle, 1984; Randich and Kuzniar, 1984). The underlying bedrock is a fractured siliceous shale from the Odanah Member of the Pierre Formation (formerly Riding Mountain Formation). The stratigraphy within the valley is variable but includes a basal, shaly sand and gravel, and a series of undefined clay-rich and silty till units locally interstratified with sands of variable thickness and extent.

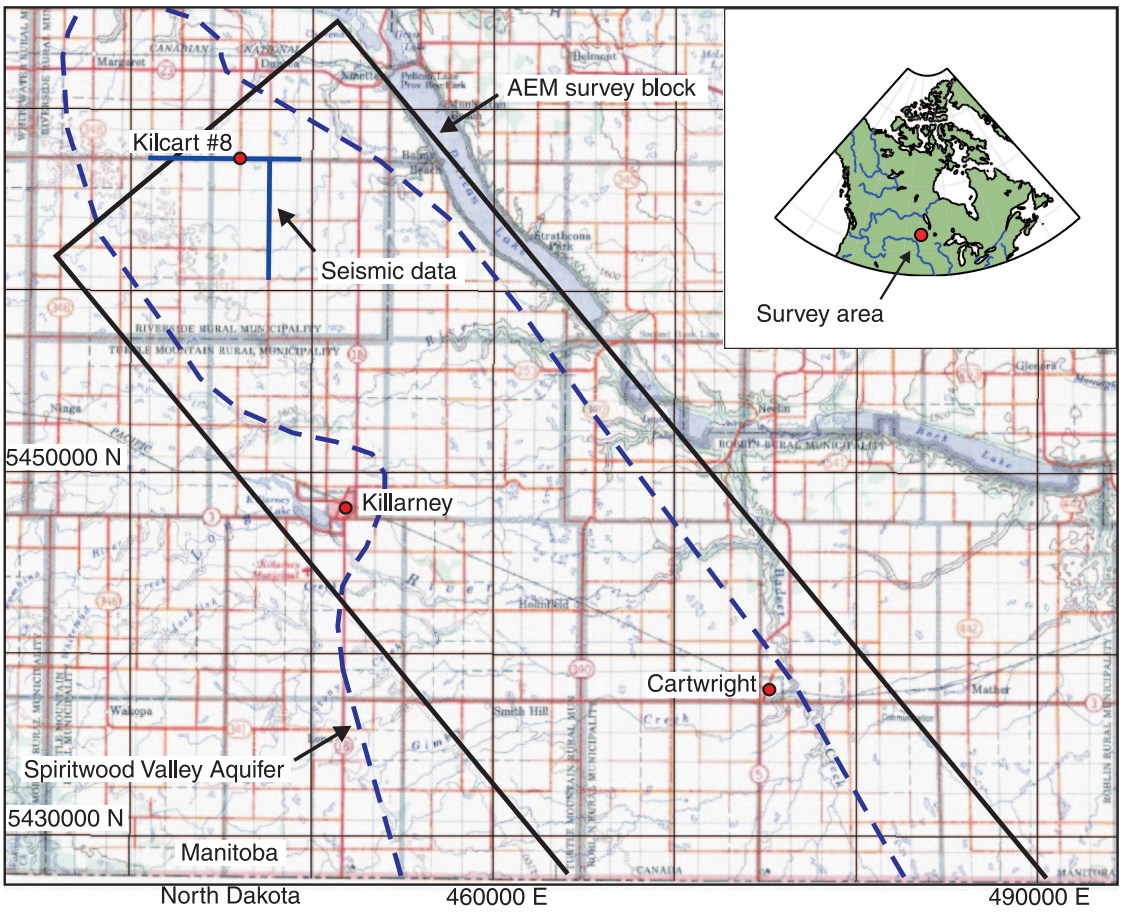

Figure 1. Outline map of the Spiritwood Valley aquifer based on overburden thickness (*modified from* Wiecek, 2009). Also illustrated are the locations of the seismic data sections, the Kilcart #8 borehole, and the AEM survey block. Inset map of Canada shows survey area.

The basal sand and gravel does not occur throughout the valley but is found within and adjacent to an incised valley at the base of the Spiritwood Valley.

Landstreamer seismic reflection data collected north of Killarney provide additional details of the subsurface geological architecture of the Spiritwood Valley (Pugin et al., 2009a, b). In addition to the broad valley architecture, the seismic data reveal a valley-within-valley morphology (Fig. 2). Within the larger Spiritwood Valley exists an approximately 800 m wide incised valley with a thalweg approximately 30 m below the bottom of the main valley. The incised valley is observed from approximately 60–100 m depth and 80–110 m depth in the different sections and appears to be overfilled with up to 30 m of stratified sediment interpreted as sand and gravel. The continuity of the incised valley and the basal sand and gravel are of significant interest for groundwater resource management in terms of groundwater access, flow, and sustainability. The occurrence of shallower, permeable inter-till sand within the vertical section may have a significant impact on aquifer recharge and sustainability.

Electrical properties

Borehole logs supplied by the Groundwater Management Section of the Manitoba Water Stewardship include both long- and short-normal resistivity data in addition to drillers' logs (Betcher, 2009, pers. comm.). The short-normal values provide an estimate of the high resistivity limit, and the long-normal values provide an estimate of the low resistivity limit. The Kilcart #8 borehole is intersected by the seismic data (Fig. 1, 2) and is located on the eastern shoulder of the incised valley (Pugin et al., 2009b). The simplified electrical section consists of three main units: till, 50 Ω m; sand and gravel, 70–200 Ω m; and shale bedrock, 50 Ω m (Fig. 3). Kilcart #8 intersects approximately 13 m of sand and gravel at approximately 46–59 m depth; no available borehole data are located within the incised valley. Other borehole data in the area support this simplified electrical property model, with the exceptions that the till is commonly observed to be slightly more conductive (40 Ω m) and the shale is observed to have resistivity as low as 30 Ωm in the

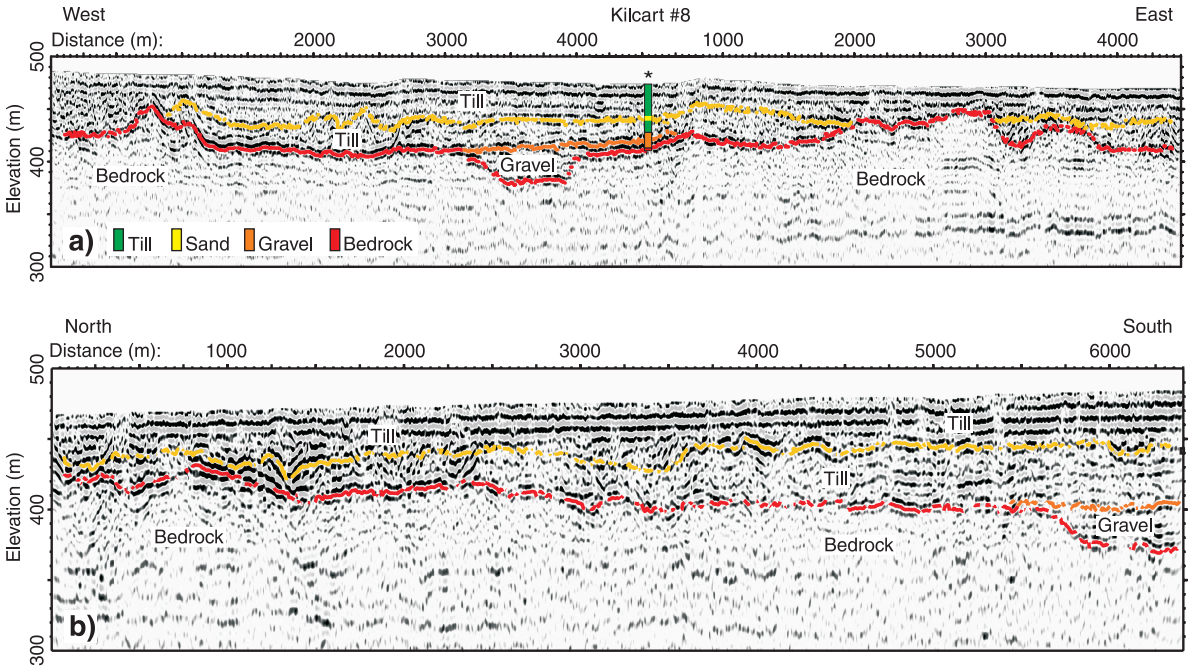

Figure 2. P-wave seismic reflection sections obtained north of Killarney, Manitoba (Pugin et al., 2009b). Approximately 8 times vertical exaggeration. The Kilcart #8 stratigraphic log is illustrated for correlation. **a)** West-east section; **b)** north-south section. *See* Figure 1 for line locations.

immediate vicinity and as low as 5 Ωm in boreholes near Brandon, Manitoba logged by the Geological Survey of Canada with an inductive tool.

Near Killarney, water conductivity within the sand and gravel unit was measured to be depth-dependent from 90–160 mS/m from 45–60 m depth (Wiecek, 2009). Using Archie's Law with an estimated formation factor of F=10 for sand/gravel, the corresponding formation resistivity is approximately 110–60 Ωm from 45–60 m depth. Within the shale bedrock, water conductivity was measured to be 400–700 mS/m (Wiecek, 2009). Again, using Archie's Law with an estimated formation factor of F=18 for shale, the corresponding formation resistivity is approximately 45–25 Ωm. These estimates are in general agreement with the borehole measurements.

AEM SYSTEM

In near-surface investigations, airborne frequency-domain electromagnetic (FEM) systems are often employed because of their large bandwidth and conductivity aperture, high spatial resolution, and strong response or discrimination capability within the shallow subsurface. As such, FEM systems have been adapted for environmental and engineering applications including some groundwater studies (e.g. Eberle and Siemon 2006; Meng et al., 2006; Smith et al., 2010). However, as demonstrated by Steuer et al. (2009), FEM surveys are limited to depths of penetration of approximately 50 m as a result of system power capabilities.

In contrast, airborne time-domain electromagnetic (TEM) systems are higher in power and offer increased depths of penetration. Design considerations for electromagnetic systems are complex (e.g. Palacky and West, 1991). However, in general, increased power is achieved at the expense of early-time data. This results in reduced bandwidth, limited conductivity aperture, and a corresponding deepening of response strength. Because of flight height, fixed-wing TEM systems lack the spatial resolution necessary to detect localized targets; therefore, power is kept high and near-surface discrimination and early-time data are sacrificed. Helicopter-borne TEM systems capitalize on the spatial resolution of the low-flying helicopter mount. Power is reduced compared to a fixed wing system, and some bandwidth is recovered. As such, helicopter-borne TEM systems are intermediate between fixed-wing TEM systems and FEM systems in depth of penetration, depth of response strength, and conductivity aperture.

Both the North Dakota borehole data and the seismic data indicate depths of the Spiritwood aquifer of up to 100–120 m and dictate the selection of a helicopter-borne TEM system. The system flown was an Aeroquest AeroTEM III (Balch et al., 2003). The AeroTEM system emits a time-varying electromagnetic signal from a horizontal loop transmitter with a triangular-bipolar current waveform (Fig. 4). The time-varying current waveform generates a

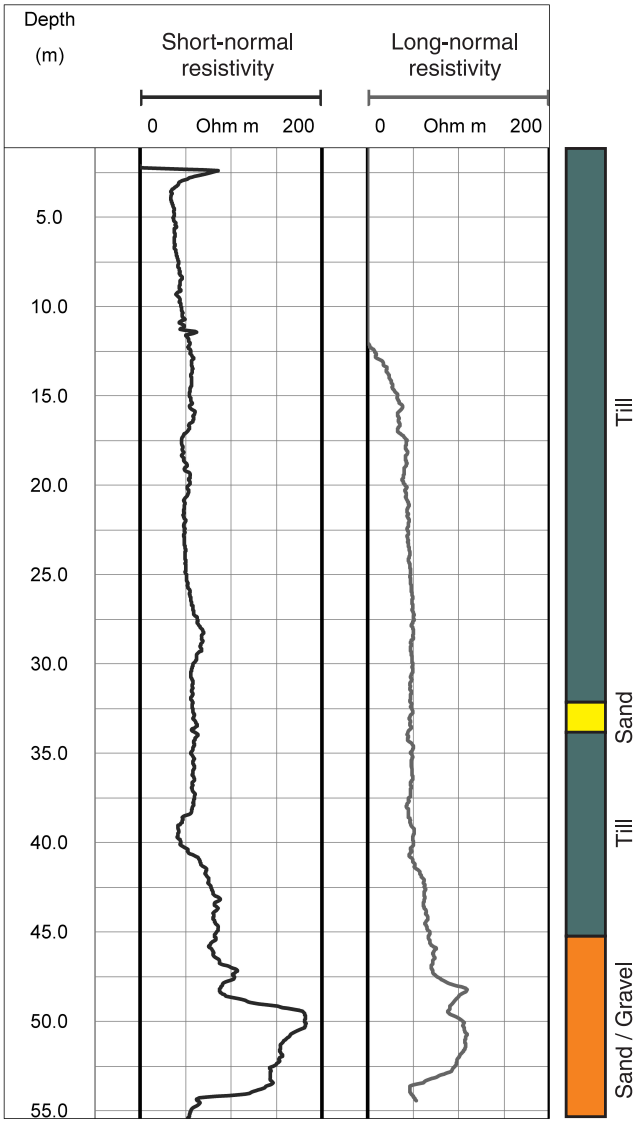

Figure 3. Long- and short-normal resistivity logs for the Kilcart #8 borehole (provided by the Groundwater Management Section of the Manitoba Water Stewardship). The stratigraphic log is a simplified interpretation of the driller's log from Kilcart #8. Plot points for the resistivity logs do not necessarily correspond to true depth. According to the driller's log, bedrock is at 59 m depth. Bedrock influence is apparent at the bottom of both resistivity logs.

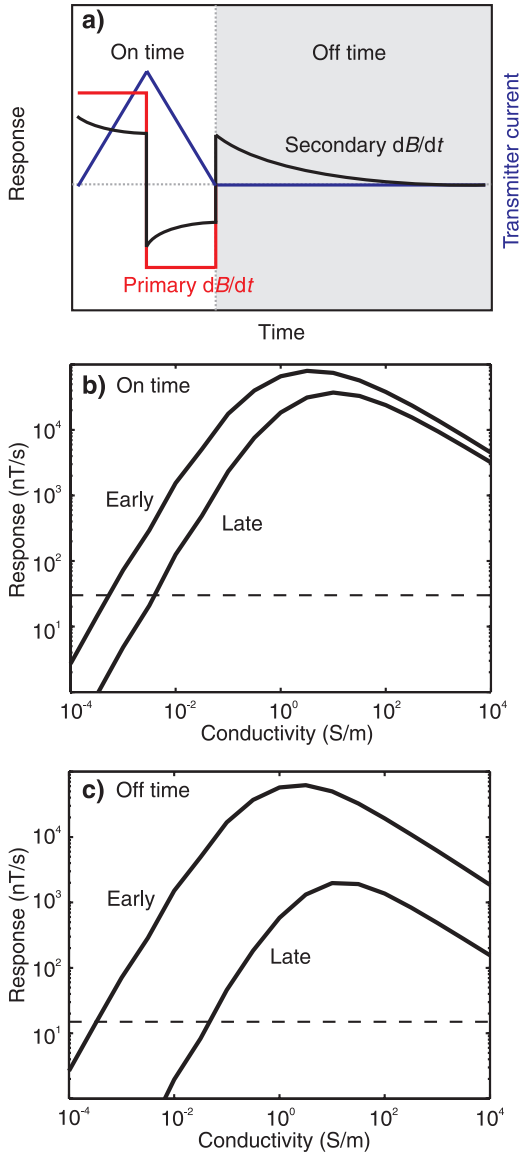

Figure 4. a) Schematic AeroTEM III transmitter waveform and response. At 90 Hz, the triangular current pulse is approximately 1.7 ms in duration. The on-time response is derived from both the up- and downslope regions of the transmitter waveform. The duration of off-time measurements is approximately 3.4 ms after transmitter turn off. **b)** On-time and **c)** off-time halfspace nomograms for the AeroTEM III system illustrating the conductivity range of peak system response of the vertical component dB_z/dt. The dashed horizontal lines represent the approximate system noise levels. Provided by Aeroquest Surveys.

Table 1. Specifications for the AeroTEM III

Data rate (Hz)	Nominal data interval (m)	Base frequency (Hz)	Pulse width (ms)	Sample frequency (kHz)	Nominal MTC (m)	Loop diameter (m)	Dipole moment (Am^2)
10	2.3	90	1.7	36	35	9	237000

time-varying primary magnetic field, which gives rise to an electric field that drives induced currents within the earth. The induced currents generate a secondary magnetic field. The system measures voltage in an induction coil sensor. The voltage is equivalent to the time rate of change of the secondary magnetic field dB/dt resulting from the induced currents. The system is a rigid concentric coil system with a symmetric response. Active bucking of the primary field allows for both on- and off-time measurements of dB_z/dt and dB_x/dt. Measured data are captured at a streamed rate of 36 kHz and are reported at a series of 16 constant-width time gates from 112.5–529.2 µs in the on time and 17 variable-width time gates from 70.1–2917.3 µs in the off time (Fig. 4). System specifications are detailed in Table 1.

A halfspace nomogram for the AeroTEM III system is illustrated in Figure 4 and is representative of the conductivity aperture. Peak system response over a halfspace occurs from approximately 1–10 S/m (1–0.1 Ω m) from early to late off time. System response falls below noise levels from approximately 0.001–0.1 S/m (1000–10 Ω m) from early to late off time. The AeroTEM III waveform is designed to generate a strong response for high conductance bodies (e.g. West et al., 1984; Smith and Annan, 2000). In comparison to the estimated material properties for the Spiritwood Valley, we see that peak system response occurs for materials that are significantly more conductive than the valley fill. Nevertheless, the estimated material properties are within the usable conductivity aperture, although interpretation of near-surface (early-time) features may be difficult, particularly if they are resistive. Similarly, interpretation of resistive features may be difficult, particularly if they are at shallow depth.

Data acquisition

The Spiritwood Valley AEM survey area is illustrated in Figure 1. The survey area is rectangular, 1062 km^2 and bounded to the south by the Canada–USA border (Table 2). Traverse lines were planned at approximately 50° azimuth at 400 m spacing. Control lines were planned at approximately 320° azimuth at 5000 m spacing. Survey geometry was designed based on a compromise between axial and lateral coverage and cost. Given the linear nature of the survey target and the relatively well-known axial direction, line spacing was increased to 400 m as opposed to the typical "mapping standard" of 200 m in order to increase coverage. Control line spacing was also increased from standard because of the secondary importance of the magnetic data (this will limit the ability to generate processed magnetic variables such as first and second vertical derivatives).

Table 2. Survey block corner co-ordinates, NAD 83 UTM Zone 14N.

Block 1		Block 2	
Easting (m)	Northing (m)	Easting (m)	Northing (m)
490720	5427700	444900	5451220
460315	5463955	436060	5462000
444900	5451220	451440	5474730
464430	5427700	460315	5463955

The survey and calibrations were flown during the period from February to March, 2010. Data acquisition and preliminary processing were carried out by Aeroquest Surveys. AEM system elevation was maintained at a nominal mean terrain clearance (MTC) of 35 ± 5 m. Navigation was performed using on-board real-time differential GPS, and aircraft height was monitored with a digital radar altimeter. A vertically mounted video camera was used to record images of the ground. In addition to the AEM data, magnetic data were acquired at a rate of 10 Hz using a Caesium vapour magnetometer. The magnetic response is likely indicative of deep crystalline bedrock and is not directly applicable for the groundwater investigation detailed here.

The survey was flown in two blocks (Table 2) and the data were merged into a single dataset by Aeroquest Surveys. The raw AEM data consist of on- and off-time decay curves for the x and z components. The raw decays were levelled for linear drifts in base level signal using high-altitude corrections (e.g. Sørensen and Auken 2004). A number of parameters can then be derived from the levelled AEM data, including the on- and off-time decay constants and the apparent conductivity.

RESULTS

Maps of final processed AEM parameters will be available through the Geological Survey of Canada as Open File reports. In addition, the AEM data will be publicly available via the Geoscience Data Repository of the Earth Sciences Sector, Natural Resources Canada.

Preliminary AEM data are illustrated in Figures 5 to 8 as a series of select off-time slices at gates 4, 7, 10 and 13 for the z component. The levelled decay curves were decimated by every 50 measurements (approximately 85 m average spacing) and then interpolated onto a 100 m regular grid. In general, the early-time data represent shallow and/or resistive features and the late-time data represent deep and/or conductive features. Good conductors generate a strong EM response with a slow decay. Strong, shallow conductors may appear early in time and be persistent into late time. Deep, strong conductors will also be persistent, but will appear later in time. In contrast, poor conductors generate a weak AEM response with a fast decay. Poor, shallow conductors will show up early in time and deep, poor conductors will show up later in time.

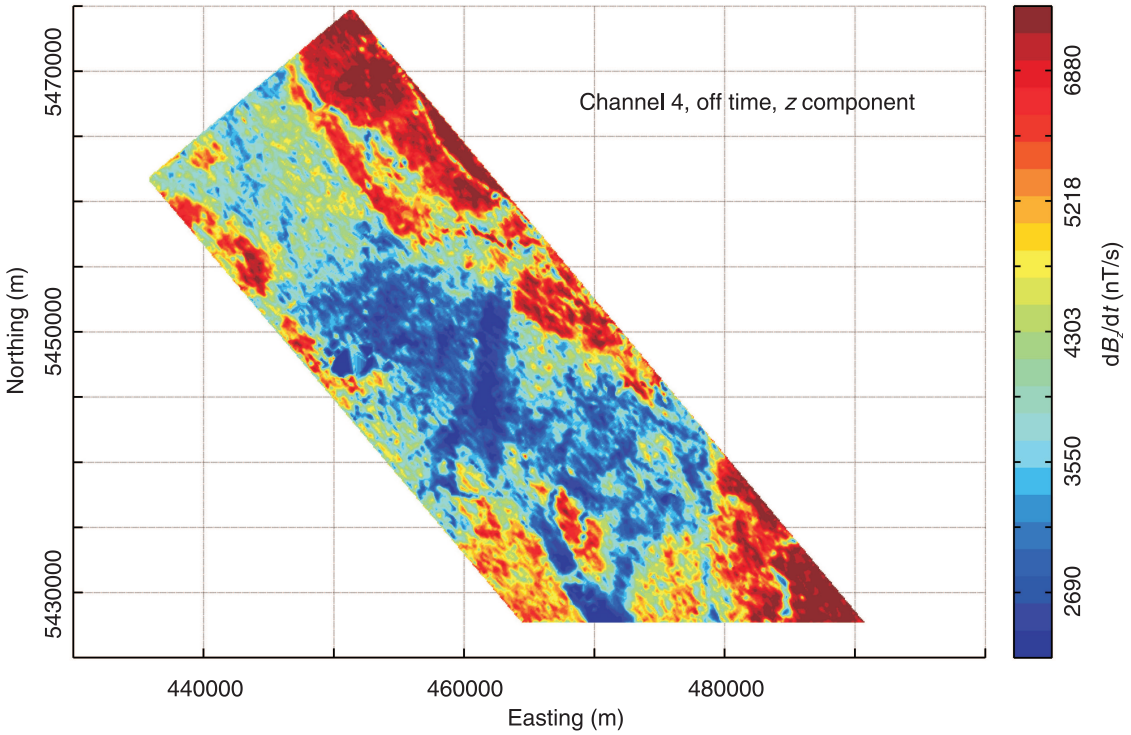

Figure 5. Channel 4 off-time response of the vertical component of the EM system at 181.2 μs after transmitter turn off. The colour scale is a normal distribution of the log-transformed decay rate resulting in compressed contrast at high and low values.

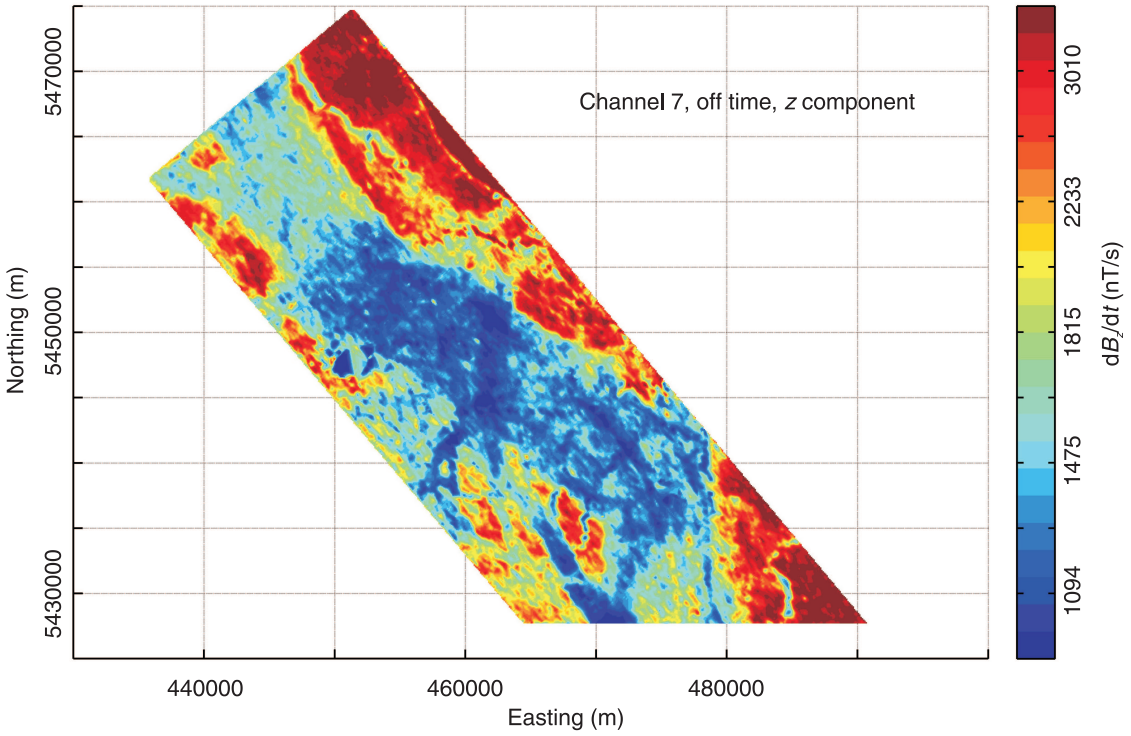

Figure 6. Channel 7 off-time response of the vertical component of the EM system at 347.9 μs after transmitter turn off. The colour scale is a normal distribution of the log-transformed decay rate resulting in compressed contrast at high and low values.

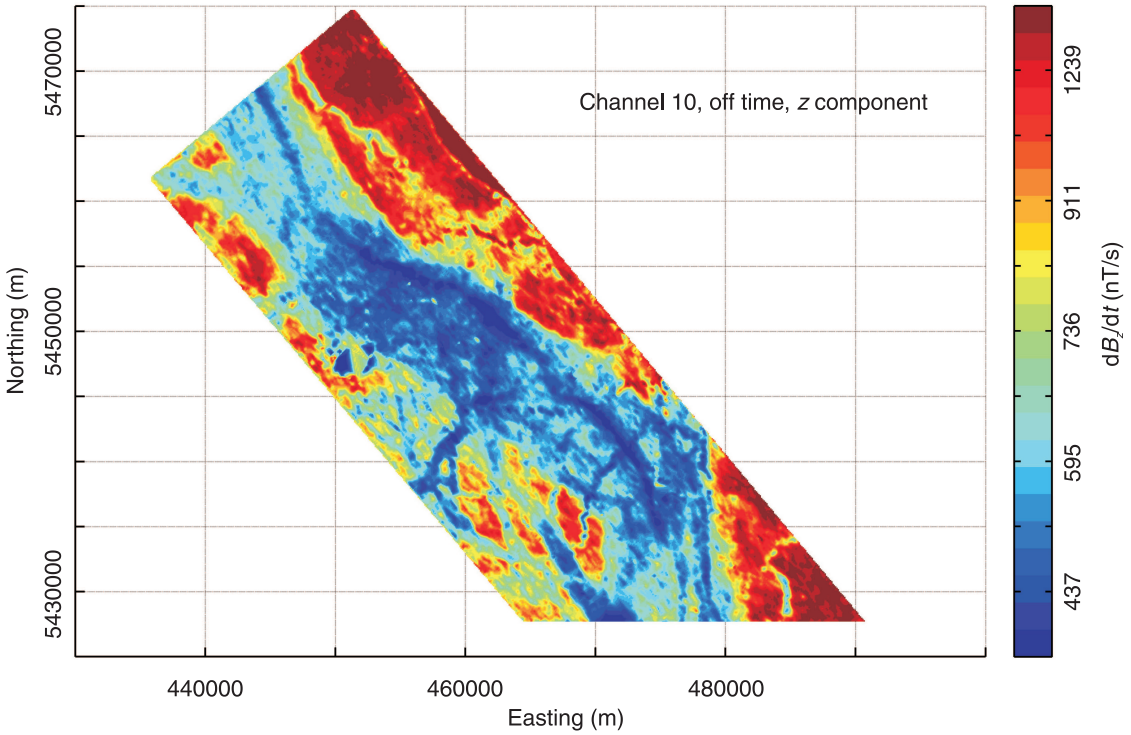

Figure 7. Channel 10 off-time response of the vertical component of the EM system at 625.6 μs after transmitter turn off. The colour scale is a normal distribution of the log-transformed decay rate resulting in compressed contrast at high and low values.

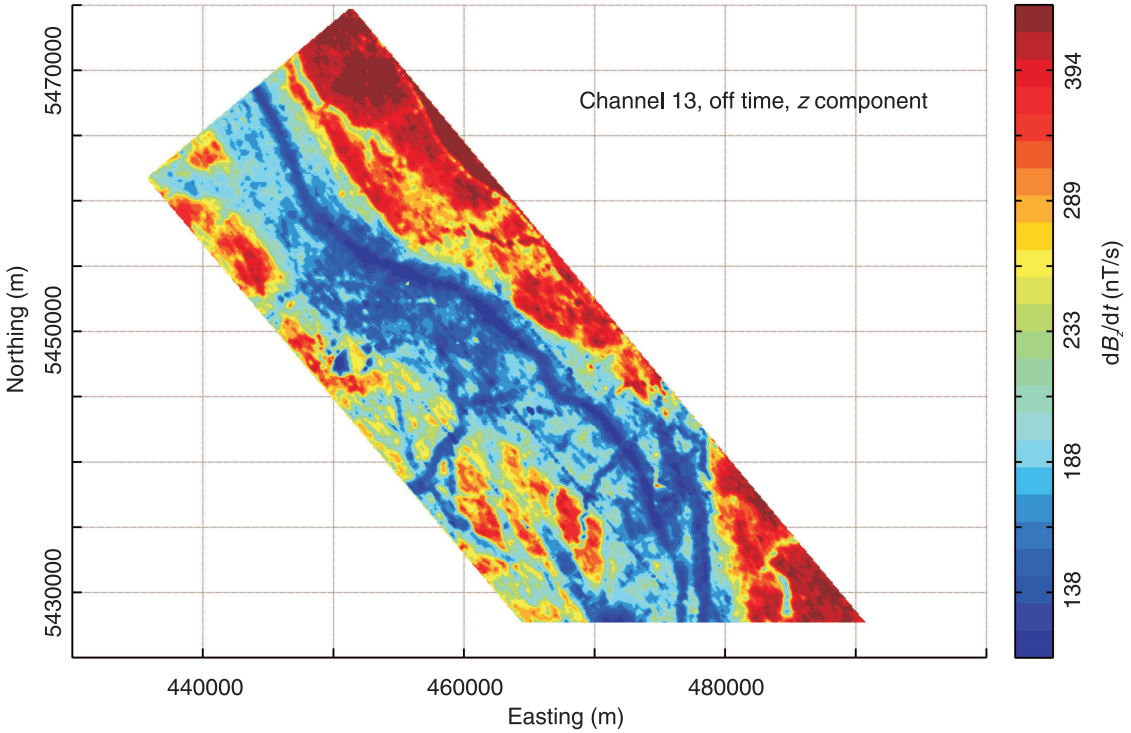

Figure 8. Channel 13 off-time response of the vertical component of the EM system at 1167.3 μs after transmitter turn off. The colour scale is a normal distribution of the log-transformed decay rate resulting in compressed contrast at high and low values.

Levelling noise (and some gridding error) is apparent in Figure 8 and is manifest as anomalous patterns parallel to the flight lines. This flight-line striping becomes more severe at even later time channels and represents variability of the system base level on a flight-by-flight basis (some striping may also be due to gridding). Cultural noise such as power lines shows up in the late channels when signal strength is weak. Conclusive identification of cultural responses is possible by examining the power line monitor and the flight track video. The communities of Killarney and Cartwright were not overflown and are represented as dead spots in the data, although on these maps we have interpolated over them.

In comparison to curves of dB/dt, more meaningful measures of material properties can be obtained through transformation of the magnetic field data to the decay constant τ and the equivalent conductance S_e. The EM decay constant was computed using an exponential fit to dB/dt at each measurement location and the equivalent conductance was computed using a fit to the synthetic response for a 100 m ×100 m horizontal plate model. For the preliminary data presented here, only the first five time channels were used in either calculation because of inconsistency of the base level at later time. The decay constant and equivalent conductance were calculated for every measurement location, decimated by every 50 measurements and then interpolated onto a 100 m regular grid. The resulting maps for the off-time z component are illustrated in Figures 9 and 10. The equivalent conductance for the on-time z component is illustrated in Figure 11.

In general, the on-time data have higher noise levels and are more difficult to interpret than the off-time data as a result of the presence of the strong primary field. Figures 10 and 11 show the similarity in character between the off- and on-time conductance, which suggests comparable information content. However, the magnitude of the apparent conductance differs by an approximate factor of 2. In fact, the collection of on-time data may allow us to extend the conductivity aperture for resistive materials via resistive-limit calculations (Smith, 2000), but the on-time data are not considered further here.

Similarly, the x-component data (not shown) have higher noise levels and are more difficult to interpret that the z-component data. Collection of x-component data can be critical for discrimination of conductor geometry, particularly for vertically-oriented features. However, for the resistivity mapping application considered here, the x component has arguably little information, especially at the level of preliminary interpretation. A slight response in τ_x is observed over the incised valley, perhaps indicative of the vertical nature of the feature compared to other geology. The equivalent conductance of the x component shows no significant response.

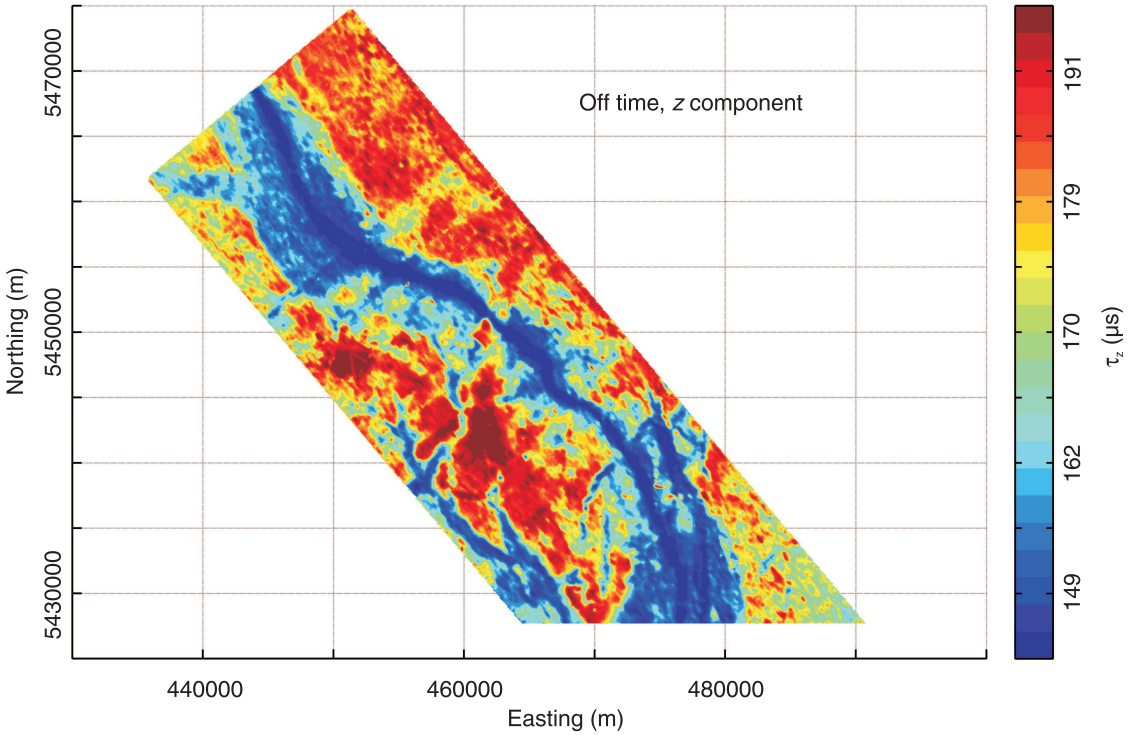

Figure 9. Off-time decay constant for the vertical component of the EM system. The colour scale is a normal distribution of the decay constant resulting in compressed contrast at high and low values.

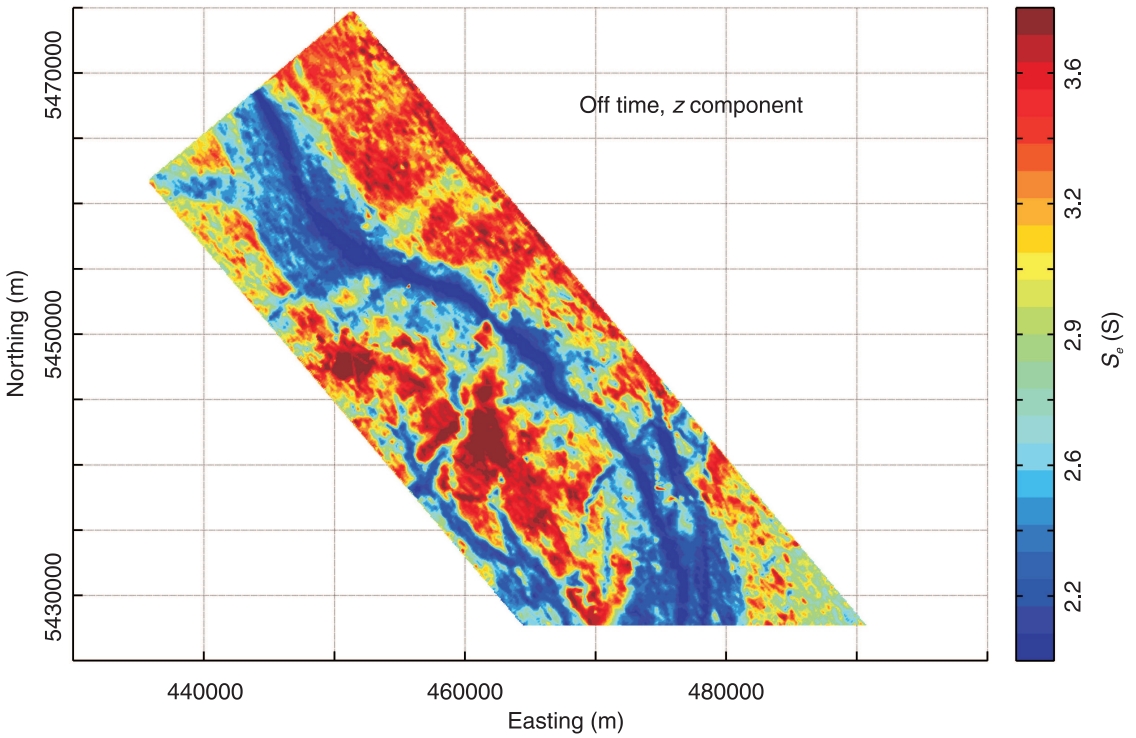

Figure 10. Off-time equivalent conductance for the vertical component of the EM system. The colour scale is a normal distribution of the conductance resulting in compressed contrast at high and low values.

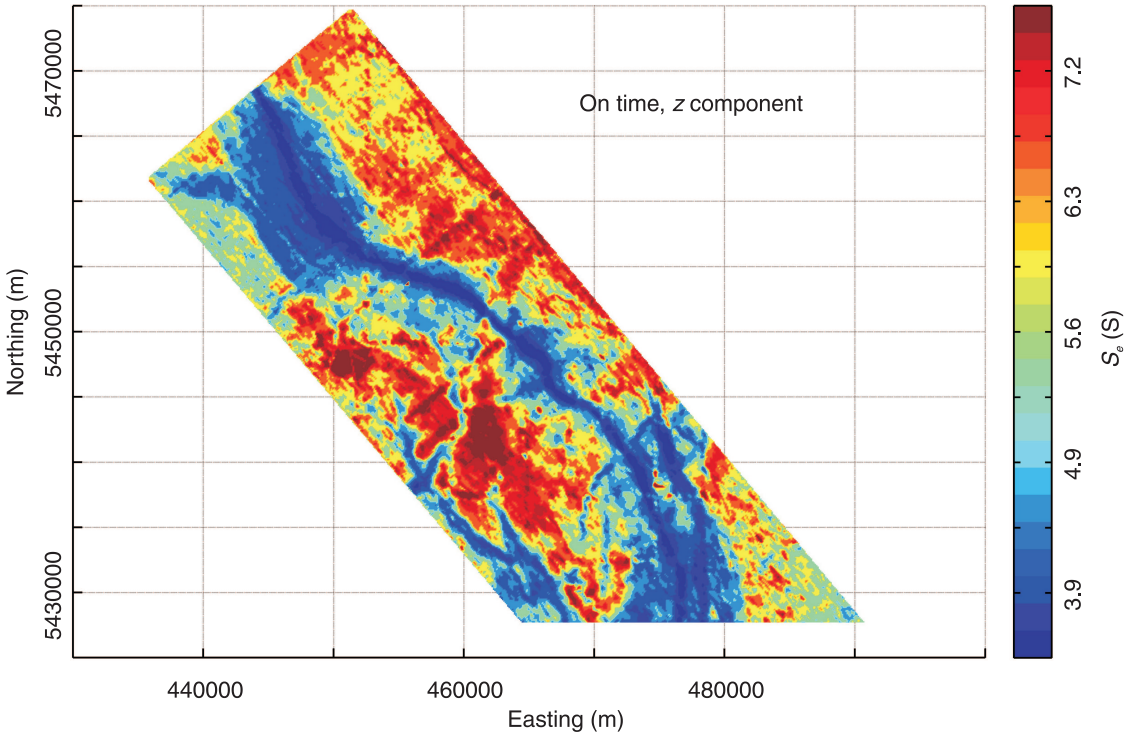

Figure 11. On-time equivalent conductance for the vertical component of the EM system. The colour scale is a normal distribution of the conductance resulting in compressed contrast at high and low values.

Preliminary interpretation

The early-time data suggest regions of relatively high (red) and low to moderate (blue and yellow) conductivity (Fig. 5). These regions are generally interpreted as the shale bedrock at the valley edges and the top layer of valley fill. At later times (Fig. 6–8), the bedrock signature is more persistent primarily because of its extent at depth. The geometry of the main valley becomes more apparent and secondary valley features of low conductivity become evident. In Figure 7, the main valley geometry is well defined and approximately 8–10 km in width. A continuous 1 km wide, low-conductivity linear feature, which is interpreted as the incised valley identified in the seismic data, can also be observed. The main valley and incised valley features are identified in Figure 12 as A and B, respectively. The incised valley geometry is most clearly defined in the channel 13 data (Fig. 8), along with a major secondary valley branch identified as C in Figure 12. It is not apparent from these data if this secondary valley feature is incised below the main valley bottom or if it continues to the north on the eastern side of Cartwright as mapped by Betcher et al. (2005). The late-time data also reveal a valley-like feature identified as D in Figure 12. This feature cannot be traced at late time, but it is apparent in early time (Fig. 5) continuing northwest and perhaps turning north near 5440000 N. Although time-slices do not correlate directly with depth, feature D may represent a dipping feature or a feature with variable vertical extent that may be deepest at its southern limit. Furthermore, feature D is aligned with a borehole drilled 5 km south of the border that that did not intercept bedrock at 140 m.

Also apparent from the time slices is a regional variability in the AEM response of the upper valley fill along the valley axis (Fig. 5, 6). The AEM response is weaker in the central region from 5440000–5455000 N indicating more resistive material (possibly sand as opposed to till). However, this interpretation is not directly corroborated by the integrated measures of the decay constant (Fig. 9) or the equivalent conductance (Fig. 10) that indicate rapidly decaying or more resistive material in the north and south. There are similar inconsistencies with the northern extent of feature D. In contrast, the incised valley has both a low amplitude of AEM response (Fig. 12), a rapid decay or low

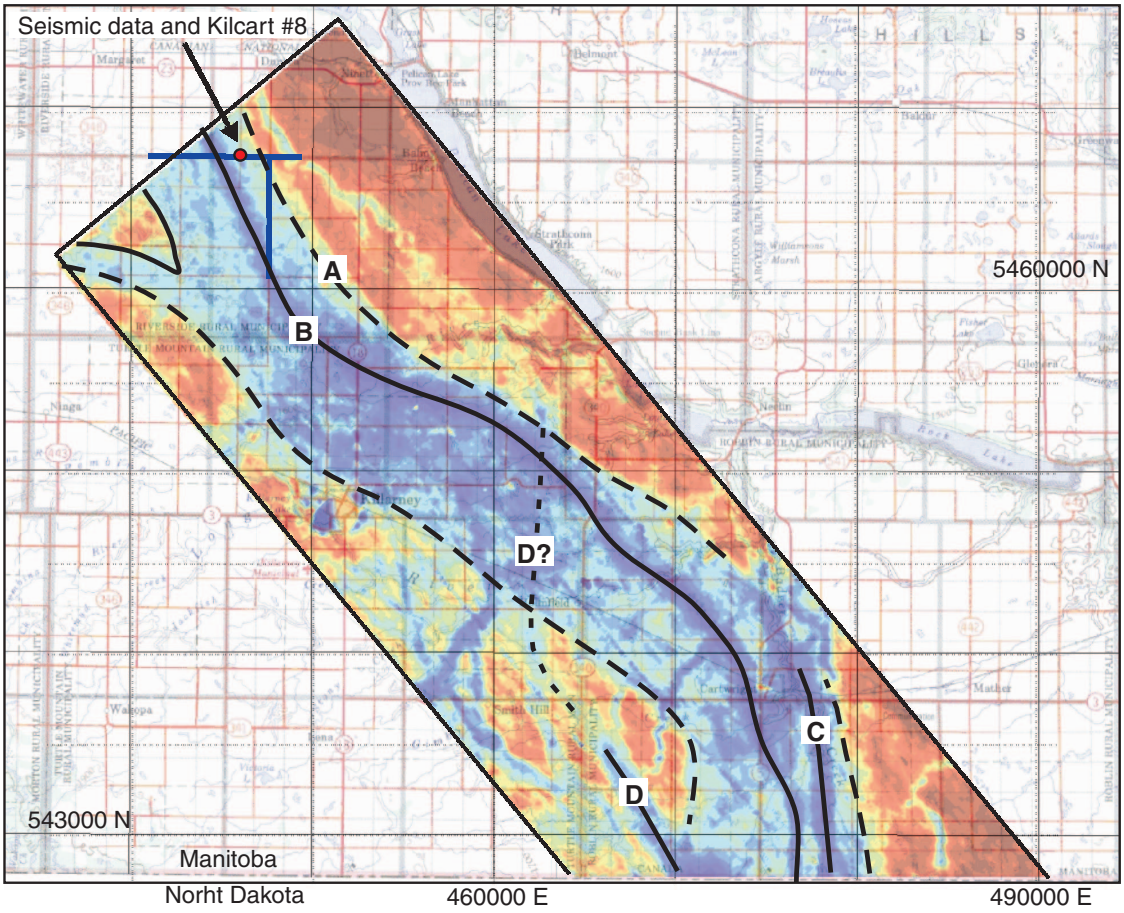

Figure 12. Interpreted features of the Spiritwood Valley aquifer system based on the AEM data. The channel 13 off-time response is overlain on the survey area map. A: Revised approximate Spiritwood Valley outline. B: Incised valley axis. C: Major secondary valley branch. D: Dipping valley.

time constant (Fig. 9), and a low equivalent conductance (Fig. 10), all of which are consistent with resistive material such as sand and gravel fill.

The AEM data and interpretation are in excellent agreement with the seismic data (Fig. 2). The incised valley as observed in the AEM response is well-aligned with the sand and gravel fill identified in both seismic sections (Fig. 12). The AEM data also confirm the bedrock high and low interpreted at the eastern end of the west-east section (Fig. 2a) and the "shoulder" location of Kilcart #8. The AEM data are not sensitive to the thin layer of sand observed in the seismic sections, but detection of thin resistors is a known limitation of inductive electromagnetic methods (e.g. Huang and Rudd, 2008).

CONCLUDING DISCUSSION

Helicopter-borne AEM data were collected over the Spiritwood Valley in southern Manitoba in order to test the applicability of time-domain electromagnetics for mapping and characterizing buried valley aquifers in the Canadian landscape. The experiment was flown by Aeroquest Surveys using the commercial AeroTEM III system. In general, there is rich information content in the data. Preliminary late-time data are contaminated by some degree of levelling noise that is variable across the survey block. Final data processing should ameliorate these issues and allow for the usage of all time channels in computing the AEM parameters of decay constant and apparent conductivity. Inclusion of late-time data will hopefully expand the limited dynamic range observed in the derived parameters, but this may be a system bandwidth limitation. The Spiritwood Valley survey represents a resistive scenario for typical TEM applications, but the sand and gravel deposits are relatively conductive aquifer materials because of their predominant shale provenance – clean sand and gravel may require an increased conductivity aperture.

These preliminary results suggest that time-domain electromagnetic surveys are a potentially valuable method of mapping buried valley aquifers in the Canadian Prairies in far greater detail that any previous techniques. For the first time, the location, scale, and secondary morphological features of the Spiritwood Valley aquifer system have been defined. The AEM data indicate a complex valley geometry with nested valley scales and variability of valley orientation and fill material. The southernmost extent of the survey suggests that three, distinct valley features cross the international border within the broader Spiritwood Valley, and that there may be only limited hydraulic connections between them. Time slices of the magnetic field decay clearly illustrate the existence of a continuous incised valley within the broader Spiritwood Valley in addition to at least two other buried valley features. The AEM data can be used to successfully map valley locations that continue to be difficult to define using seismic and borehole methods. Furthermore, the AEM data suggest a marked difference in fill material between the main and incised valleys. This observation may improve understanding of the spatial variability of valley fill that has complicated the positioning of groundwater monitoring wells and hydraulic modelling of buried valleys.

The AEM data are in excellent agreement with seismic reflection data collected inside the survey block, and further integration of these data types, along with borehole information, is promising. Acquisition of additional seismic reflection data is planned along with ground-based electrical resistivity experiments. Such data will allow for calibration of AEM results in terms of depth and electrical properties. Calibration will be critical during the advanced processing stages of conductivity-depth imaging and full inversion. The goals of advanced processing will be accurate placement of information with depth, and better understanding of material properties or better characterization of fill materials.

ACKNOWLEDGMENTS

The AEM survey was made possible through the Groundwater Geoscience program of the Geological Survey of Canada, Natural Resources Canada. Many people were instrumental in the planning, contracting, and execution of the experiment. In particular, H. Crow co-ordinated borehole data; R. Dumont, V. Holmes, P. Keating, and W. Miles were critical in survey planning and contracting; K. Brewer performed the technical inspection; and B. Betcher of the Groundwater Management Section of the Manitoba Water Stewardship provided borehole information and consulting reports. J. Hunter and P. Keating provided constructive reviews.

REFERENCES

Abraham, J.D., Cannia, J.C., Peterson, S.M., Smith, B.D., Minsley, B.J., and Bedrosian, P.A., 2010. Using airborne geophysical surveys to improve groundwater resource management models; *in* Symposium on the Application of Geophysics to Environmental and Engineering Problems; p. 309–314, Environmental and Engineering Geophysical Society.

Auken, E., Christiansen, A.V., Jacobsen, L.H., and Sørensen, K.I., 2008. A resolution study of buried valleys using laterally constrained inversion of TEM data; Journal of Applied Geophysics, v. 65, p. 10–20. doi:10.1016/j.jappgeo.2008.03.003

Balch, S.J., Boyko, W.P., and Paterson, N.R., 2003. The AeroTEM airborne electromagnetic system; Leading Edge (Tulsa, Okla.), v. 22, p. 562–566. doi:10.1190/1.1587679

Betcher, R.N., Matile, G., and Keller, G., 2005. Yes Virginia, there are buried valley aquifers in Manitoba; *in* Proceedings of the 58th Canadian Geotechnical Conference, Saskatoon, Canadian Geotechnical Society, 6E-519, Saskatoon, SK.

Bluemle, J.P., 1984. Geology of Towner County, North Dakota; County Groundwater Studies 36, Part I, North Dakota State Water Commission.

Eberle, D.G. and Siemon, B., 2006. Identification of buried valleys using the BGR helicopter-borne geophysical system; Near Surface Geophysics, v. 4, p. 125–133.

Gabriel, G., Kirsch, R., Siemon, B., and Wiederhold, H., 2003. Geophysical Investigation of buried Pleistocene subglacial valleys in Northern Germany; Journal of Applied Geophysics, v. 53, p. 159–180. doi:10.1016/j.jappgeo.2003.08.005

Huang, H. and Rudd, J., 2008. Conductivity-depth imaging of helicopter-borne TEM data based on a pseudolayer half-space model; Geophysics, v. 73, p. F115–F120. doi:10.1190/1.2904984

Jørgensen, F. and Sandersen, P.B.E., 2009. Buried Valley mapping in Denmark: evaluating mapping method constraints and the importance of data density; Zeitschrift der Deutschen Gesellschaft für Geowissenschaften, v. 160, p. 211–223. doi:10.1127/1860-1804/2009/0160-0211

Martinez, K., Lo, B., Ploug, C., Pitcher, D., and Tishin, P., 2008. Water resources applications with the VTEM system; *in* Proceedings of the 5th International Conference on Airborne Electromagnetics, 08-01. Haikko Manor, Finland.

Meng, Q., Hui, H., and Yu, Q., 2006. The application of an airborne electromagnetic system in groundwater resource and salinization studies in Jilan, China; Journal of Environmental & Engineering Geophysics, v. 11, p. 103–109. doi:10.2113/JEEG11.2.103

Palacky, G.J. and West, G.F., 1991. Airborne electromagnetic methods; *in* Electromagnetic Methods in Applied Geophysics, Society of Exploration Geophysicists, v. 2, p. 811–880.

Pugin, A.J., Pullan, S.E., Hinton, M.J., Cartwright, T., Douma, M., and Burns, R.A., 2009a. Mapping buried valley aquifers in SW Manitoba using a vibrating source/landstreamer seismic reflection system; *in* Symposium on the Application of Geophysics to Environmental and Engineering Problems; Environmental and Engineering Geophysical Society, p. 586–595.

Pugin, A.J., Pullan, S.E., Hunter, J.A., and Oldenborger, G.A., 2009b. Hydrogeological prospecting using P- and S-wave landstreamer seismic reflection methods; Near Surface Geophysics, v. 7, p. 315–327.

Randich, P.G. and Kuzniar, R.L., 1984. Geology of Towner County, North Dakota; County Groundwater Studies 36, Part III, North Dakota State Water Commission.

Russell, H.A.J., Hinton, M.J., van der Kamp, G., and Sharpe, D., 2004. An overview of the architecture, sedimentology and hydrogeology of buried-valley aquifers in Canada; *in* Proceedings of the 57th Canadian Geotechnical Conference, Canadian Geotechnical Society, 24–27 October, p. 26–33.

Sharpe, D.R., Hinton, M.J., Russell, H.A.J., and Desbarats, A.J., 2002. The need for basin analysis in regional hydrogeological studies: Oak Ridges Moraine, Southern Ontario; Geoscience Canada, v. 29, p. 3–20.

Shaver, R.B. and Pusc, S.W., 1992. Hydraulic barriers in Pleistocene buried-valley aquifers; Ground Water, v. 30, p. 21–28. doi:10.1111/j.1745-6584.1992.tb00807.x

Smith, R.S., 2000. The realizable resistive limit: A new concept for mapping geological features spanning a broad range of conductances; Geophysics, v. 65, p. 1124–1127. doi:10.1190/1.1444805

Smith, R.S. and Annan, A.P., 2000. Using an induction coil sensor to indirectly measure the B-field response in the bandwidth of the transient electromagnetic method; Geophysics, v. 65, p. 1489–1494. doi:10.1190/1.1444837

Smith, R.S., O'Connell, M.D., and Poulsen, L.H., 2004. Using airborne electromagnetics surveys to investigate the hydrogeology of an area near Nyborg, Denmark; Near Surface Geophysics, v. 2, no. 3, p. 123–130.

Smith, B.D., Abraham, J.D., and Lundstrom, S.C., 2010. Airborne electromagnetic surveys by the U.S. Geological Survey over concealed glacial aquifers, central United States; Environmental and Engineering Geophysical Society, Symposium on the Application of Geophysics to Environmental and Engineering Problems, p. 126–137.

Sørensen, K.I. and Auken, E., 2004. SkyTEM – a new high-resolution helicopter transient electromagnetic system; Exploration Geophysics, v. 35, p. 191–199.

Steuer, A., Siemon, B., and Auken, E., 2009. A comparison of helicopter-borne electromagnetics in frequency- and time-domain at the Cuxhaven valley in Northern Germany; Journal of Applied Geophysics, v. 67, p. 194–205. doi:10.1016/j.jappgeo.2007.07.001

Walker, S. and Rudd, J., 2008. Airborne resistivity mapping with helicopter TEM: An oil sands case study; *in* 5th International Conference on Airborne Electromagnetics, 06-03, Haikko Manor, Finland.

West, G.F., Macnae, J.C., and LaMontagne, Y., 1984. A time-domain EM system measuring the step response of the ground; Geophysics, v. 49, p. 1010–1026. doi:10.1190/1.1441716

Wiecek, S., 2009. Municipality of Killarney – Turtle Mountain groundwater assessment study; W.L. Gibbons & Associates Inc.

Winter, T.C., Benson, R.D., Engberg, R.A., Wiche, G.J., Emerson, D.G., Crosby, O.A., and Miller, J.E., 1984. Synopsis of ground-water and surface-water resources of North Dakota; United States Geological Survey, Open File Report 84-732.

Geological Survey of Canada Project AM1002-AMI